JOURNAL OF COMPUTATIONAL PHYSICS 93, 343–359 (1991)

High Accuracy Solutions of Incompressible Navier–Stokes Equations

MURLI M. GUPTA

Department of Mathematics, The George Washington University, Washington, DC 20052

Received February 21, 1989; revised February 8, 1990

In recent years we have developed high accuracy finite difference approximations for partial differential equations of elliptic type, with particular emphasis on the convection–diffusion equation. These approximations are of compact type, have a local truncation error of fourth order, and allow the use of standard iterative schemes to solve the resulting systems of algebraic equations. In this paper, we extend these high accuracy approximations to the solution of Navier–Stokes equations. Solutions are obtained for the model problem of driven cavity and are compared with solutions obtained using other approximations and those obtained by other authors. It is discovered that the high order approximations do indeed produce high accuracy solutions and have a potential for use in solving important problems of viscous fluid flows.

INTRODUCTION

The basic model for the fluid dynamics phenomena representing two- and three-dimensional flows of an incompressible viscous fluid is given by the Navier–Stokes equations that represent the conservation of mass, momentum, and energy. These equations are highly nonlinear and are very difficult to solve, especially when the approximate solutions are required to have a high accuracy. A related problem is that of obtaining highly accurate solutions of the convection–diffusion equation, especially when convection is the dominating phenomena.

Prior to the last decade, many researchers examined a number of first- and second-order finite difference and finite element methods that were accurate and stable. In the area of finite difference methods, it was discovered that although central difference approximations were locally second-order accurate they often suffered from computational instability and the resulting solutions exhibited non-physical oscillations. The upwind difference approximations were computationally stable, although only first-order accurate, and the resulting solutions exhibited the effects of artificial viscosity. The second-order upwind methods were no better and the higher order finite difference methods of conventional type were computationally inefficient.

An exception has been found in the high order finite difference schemes of compact type that are computationally efficient and stable and yield highly accurate

0021-9991/91 $3.00

numerical solutions at least for the linear and quasilinear partial differential equations. Simplest version of such compact schemes is given for the Poisson equation

$$\partial^2 u/\partial x^2 + \partial^2 u/\partial y^2 = f(x, y)$$

which can be discretized at a grid point (x, y) by a nine-point finite difference approximation:

$$4[u_1 + u_2 + u_3 + u_4] + u_5 + u_6 + u_7 + u_8 - 20u_0 = \tfrac{1}{2}h^2[f_1 + f_2 + f_3 + f_4 + 8f_0].$$

(See Fig. 1 for the computational stencil.) This approximation was named Mehrstellenverfahren by Collatz [3] (see also [10]). It has a local truncation error of order h^4 and is an approximation of compact type as it involves only the eight nearest neighbours of the point (x, y). This type of approximations have been obtained for other elliptic equations by many researchers: the Hodie schemes of Lynch and Rice [14] (see also [2]), the OCI schemes of Berger *et al.* [1], and the SCHOS schemes of Gupta *et al.* [12, 13] all reduce to the above difference approximation when applied to the Poisson equation. Similar compact schemes of order h^6 have also been obtained [15].

The compact schemes of Gupta *et al.* (called SCHOS in the earlier papers) were applied to the convection–diffusion equations in particular and were found to yield high accuracy when applied to a large number of test problems including problems of convection-dominated flows [12]. In this paper, we extend these finite difference schemes to the Navier–Stokes equations. As a test of this method, we solve the model problem of a lid driven cavity for small to moderate values of the Reynolds number and compare our numerical solutions with the highly accurate benchmark solutions available in the literature. We find that our method yields high accuracy even though we use a relatively coarse grid.

In the next section we describe the fourth-order compact difference schemes for the convection–diffusion equation and for the Navier–Stokes equations. The model problem of the lid-driven cavity is described in the following section with detailed comparisons of our solutions with the existing solutions in the literature.

Finite Difference Approximations

Consider the following steady convection–diffusion equation:

$$\partial^2 u/\partial x^2 + \partial^2 u/\partial y^2 + p(x, y)\,\partial u/\partial x + q(x, y)\,\partial u/\partial y = f(x, y). \tag{1}$$

Finite difference approximations of Eq. (1) at the grid point (x, y) are obtained in terms of the function values of u, p, q, and f at (x, y) and its neighbours. Assuming a uniform grid in both x and y directions, we number the grid points (x, y), $(x+h, y)$, $(x, y+h)$, $(x-h, y)$, $(x, y-h)$, $(x+h, y+h)$, $(x-h, y+h)$, $(x-h, y-h)$, $(x+h, y-h)$ as 0, 1, 2, 3, 4, 5, 6, 7, 8, respectively (see Fig. 1). In writing the finite difference approximations a single subscript "j" denotes the corresponding function value at the grid point numbered "j."

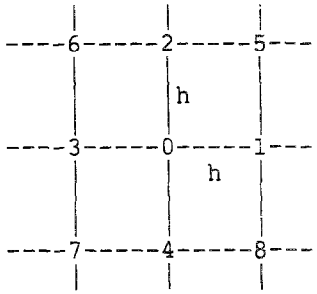

FIG. 1. Computational stencil.

The usual central difference approximation of Eq. (1) at the point (x, y) is given by

$$[u_1+u_2+u_3+u_4-4u_0]+\tfrac{1}{2}p_0h(u_1-u_3)+\tfrac{1}{2}q_0h(u_2-u_4)=h^2f_0. \tag{2}$$

This approximation is obtained by replacing all derivatives in Eq. (1) by central differences that have truncation errors of second order. A high accuracy approximation of Eq. (1) at the grid point (x, y) is given by

$$\begin{aligned} &c_1u_1+c_2u_2+c_3u_3+c_4u_4+c_5u_5+c_6u_6+c_7u_7+c_8u_8-c_0u_0\\ &\quad=\tfrac{1}{2}h^2[f_1+f_2+f_3+f_4+8f_0]+\tfrac{1}{4}h^3[p_0(f_1-f_3)+q_0(f_2-f_4)], \end{aligned} \tag{3}$$

where,

$$\begin{aligned} c_1&=4+h/4(4p_0+3p_1+p_2-p_3+p_4)+h^2/8[4p_0^2+p_0(p_1-p_3)+q_0(p_2-p_4)],\\ c_2&=4+h/4(4q_0+q_1+3q_2+q_3-q_4)+h^2/8[4q_0^2+p_0(q_1-q_3)+q_0(q_2-q_4)],\\ c_3&=4-h/4(4p_0-p_1+p_2+3p_3+p_4)+h^2/8[4p_0^2-p_0(p_1-p_3)-q_0(p_2-p_4)],\\ c_4&=4-h/4(4q_0+q_1-q_2+q_3+3q_4)+h^2/8[4q_0^2-p_0(q_1-q_3)-q_0(q_2-q_4)],\\ c_5&=1+h/2(p_0+q_0)+h/8(q_1+p_2-q_3-p_4)+p_0q_0h^2/4,\\ c_6&=1-h/2(p_0-q_0)-h/8(q_1+p_2-q_3-p_4)-p_0q_0h^2/4,\\ c_7&=1-h/2(p_0+q_0)+h/8(q_1+p_2-q_3-p_4)+p_0q_0h^2/4,\\ c_8&=1+h/2(p_0-q_0)-h/8(q_1+p_2-q_3-p_4)-p_0q_0h^2/4,\\ c_0&=20+h^2(p_0^2+q_0^2)+h(p_1-p_3)+h(q_2-q_4). \end{aligned} \tag{4}$$

This approximation is of compact type as it involves only the nine grid values of u at the point (x, y) and its eight nearest neighbors (see Fig. 1). This approximation has a local truncation error of order h^4. Detailed derivation of this approximation is given by Gupta *et al.* [12]. (This approximation has recently been rediscovered by Dennis and Hudson [21].) Similar high order approximations for general second order elliptic equations are given in [13]. Other compact approximations of this type have been obtained for the Poisson equation [10], the

Helmholtz equation [15], and the biharmonic equation [19]. Results of computations with a large number of test problems have been reported in the cited papers and in each case these compact schemes are found to yield highly accurate numerical solutions. Moreover, the accuracy improves rapidly, consistent with the local truncation error, as the mesh is refined.

The Navier–Stokes equations representing the two-dimensional steady flow of an incompressible viscous fluid are given in streamfunction-vorticity form as follows:

$$\partial^2\psi/\partial x^2 + \partial^2\psi/\partial y^2 = -\zeta \tag{5}$$

$$\partial^2\zeta/\partial x^2 + \partial^2\zeta/\partial y^2 - \mathrm{Re}(u\,\partial\zeta/\partial x + v\,\partial\zeta/\partial y) = 0 \tag{6}$$

$$u = \partial\psi/\partial y, \qquad v = -\partial\psi/\partial x. \tag{7}$$

Here ψ is the streamfunction, ζ the vorticity; u, v are the velocities; Re is the non-dimensional Reynolds number.

The streamfunction equation (5) is a special case of Eq. (1). The fourth-order compact approximation for this equation may be obtained by putting $u = \psi, f = -\zeta$ and $p(x, y) = 0$, $q(x, y) = 0$ in Eq. (3):

$$4[\psi_1 + \psi_2 + \psi_3 + \psi_4] + \psi_5 + \psi_6 + \psi_7 + \psi_8 - 20\psi_0 = -\tfrac{1}{2}h^2[\zeta_1 + \zeta_2 + \zeta_3 + \zeta_4 + 8\zeta_0]. \tag{8}$$

The vorticity equation (6) is also a special case of Eq. (1) and the fourth-order approximation in this case may be obtained by putting $u = \zeta$, $f = 0$ and $p(x, y) = -\mathrm{Re}\,u(x, y)$, $q(x, y) = -\mathrm{Re}\,v(x, y)$ in Eqs. (3) and (4):

$$\sum_{i=1}^{8} c_i\zeta_i - c_0\zeta_0 = 0, \tag{9}$$

where

$$\begin{aligned}
c_1 &= 4 - \mathrm{Re}\,h/4(4u_0 + 3u_1 + u_2 - u_3 + u_4) \\
&\quad + (\mathrm{Re}\,h)^2/8[4u_0^2 + u_0(u_1 - u_3) + v_0(u_2 - u_4)], \\
c_2 &= 4 - \mathrm{Re}\,h/4(4v_0 + v_1 + 3v_2 + v_3 - v_4) + (\mathrm{Re}\,h)^2/8[4v_0^2 + u_0(v_1 - v_3) + v_0(v_2 - v_4)], \\
c_3 &= 4 + \mathrm{Re}\,h/4(4u_0 - u_1 + u_2 + 3u_3 + u_4) \\
&\quad + (\mathrm{Re}\,h)^2/8[4u_0^2 - u_0(u_1 - u_3) - v_0(u_2 - u_4)], \\
c_4 &= 4 + \mathrm{Re}\,h/4(4v_0 + v_1 - v_2 + v_3 + 3v_4) + (\mathrm{Re}\,h)^2/8[4v_0^2 - u_0(v_1 - v_3) - v_0(v_2 - v_4)], \\
c_5 &= 1 - \mathrm{Re}\,h/2(u_0 + v_0) - \mathrm{Re}\,h/8(v_1 + u_2 - v_3 - u_4) + (\mathrm{Re}\,h)^2\,u_0v_0/4, \\
c_6 &= 1 + \mathrm{Re}\,h/2(u_0 - v_0) + \mathrm{Re}\,h/8(v_1 + u_2 - v_3 - u_4) - (\mathrm{Re}\,h)^2\,u_0v_0/4, \\
c_7 &= 1 + \mathrm{Re}\,h/2(u_0 + v_0) - \mathrm{Re}\,h/8(v_1 + u_2 - v_3 - u_4) + (\mathrm{Re}\,h)^2\,u_0v_0/4, \\
c_8 &= 1 - \mathrm{Re}\,h/2(u_0 - v_0) + \mathrm{Re}\,h/8(v_1 + u_2 - v_3 - u_4) - (\mathrm{Re}\,h)^2\,u_0v_0/4, \\
c_0 &= 20 + (\mathrm{Re}\,h)^2\,(u_0^2 + v_0^2) - \mathrm{Re}\,h(u_1 - u_3) - \mathrm{Re}\,h(v_2 - v_4).
\end{aligned} \tag{10}$$

The velocities u, v at a grid point (x, y) are calculated from the discrete approximations of Eq. (7). The typical second-order central difference approximations for the velocities are:

$$u_0 = (\psi_2 - \psi_4)/2h, \qquad v_0 = (\psi_3 - \psi_1)/2h. \tag{11}$$

High order approximations for the velocities u, v can also be defined. We [10] earlier derived some high accuracy compact approximations for the gradients of the solution of Poisson equations. As the streamfunction equation (5) is a Poisson equation in ψ, high accuracy approximations for the gradients $\partial\psi/\partial x$, $\partial\psi/\partial y$ can be obtained from [10], and corresponding approximations for the velocities are given below. (For details of the derivation, see the cited reference.) The following approximations are compact and have a local truncation error of order h^4:

$$\begin{aligned} u_0 &= (\psi_2 - \psi_4)/3h + (\psi_5 + \psi_6 - \psi_7 - \psi_8)/12h + h(\zeta_2 - \zeta_4)/12 \\ v_0 &= (\psi_3 - \psi_1)/3h - (\psi_5 - \psi_6 - \psi_7 + \psi_8)/12h + h(\zeta_3 - \zeta_1)/12. \end{aligned} \tag{12}$$

Model Problem

As a model problem, we consider the steady flow of an incompressible viscous fluid in a square cavity ($0 \leqslant x \leqslant 1$, $0 \leqslant y \leqslant 1$). The flow is induced by the sliding motion of the top wall ($y = 1$) from right to left and is described by the Navier–Stokes equations (5)–(7). The boundary conditions are those of no slip: on the stationary walls $u = 0$ and $v = 0$; on the sliding wall $u = -1$ and $v = 0$ (see Fig. 2).

A large number of investigators have used this model problem to test new schemes and solution methods (see, for example, [4–9, 11, 17, 18, 20, 22] and references given therein). Highly accurate benchmark solutions of this problem are available in the literature. In particular, Ghia *et al.* [7] obtained highly accurate solutions using 256×256 grids for $100 \leqslant \mathrm{Re} \leqslant 10{,}000$. Schreiber and Keller [17] solved this problem using a continuation method on a sequence of grids including an 180×180 grid; Goodrich and Soh [8] used a streamfunction algorithm on a 65×65 grid. These solutions facilitate comparison and assessment of new solution techniques. Experimental and numerical work on the three-dimensional cavity has been reported by Freitas *et al.* [4, 5].

In order to solve the driven cavity problem, we replace the Navier–Stokes equations (5)–(6) by the finite difference approximations given in Eqs. (8)–(10). The velocities, defined in Eq. (7), are calculated using either the second-order approximations (11) or the fourth-order compact approximations (12) in order to compare the effectiveness of these approximations. The unit square is covered by a grid of uniform mesh width h ($h = 1/N$). The discrete approximations (8), (9) are written at each of the $(N-1)^2$ interior grid points. Zero values are prescribed for ψ on the boundary; vorticity ζ on the boundary is obtained using the Jensen

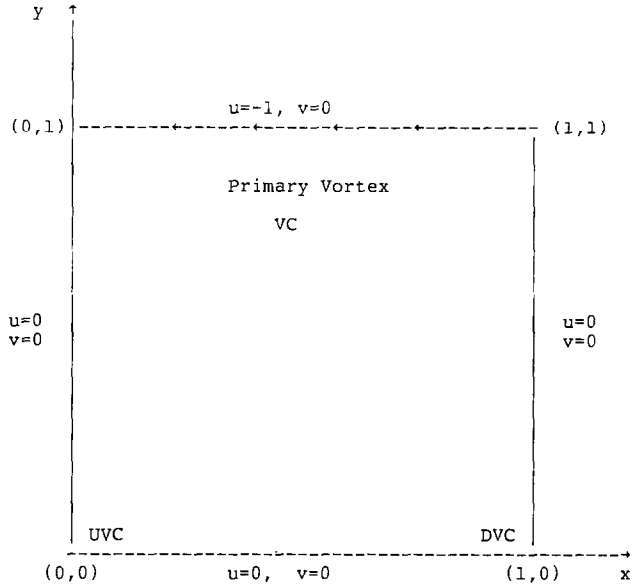

FIG. 2. Driven cavity problem.

formula [11, 16]: on the stationary walls, we define $\zeta_0 = (-8\psi_1 + \psi_2)/2h^2$; on the sliding wall $y = 1$, we define $\zeta_0 = (-8\psi_1 + \psi_2)/2h^2 + 3/h$. Here the subscript "0" denotes a grid point on the boundary; the points "1," "2" lie inside the flow region such that the points 0, 1, 2 all lie on the straight line normal to the boundary (see Fig. 3). These approximations have local truncation error of second order. Higher order approximations could also be defined for obtaining boundary values of ζ; it is anticipated that the impact on the accuracy of the computed solutions would be marginal. These and other boundary approximations for vorticity were studied in detail by Gupta and Manohar [11] (see also Gajjar [6]).

An inner–outer iteration procedure is utilized to obtain the numerical solutions. At each outer iteration, the linear systems from the discrete streamfunction and vorticity equations are solved iteratively. We solved these linear systems using point-SOR iteration with the relaxation parameters 1.7 and 1.2, respectively. The inner iterations are allowed no more than a present number (usually 10) of iterations. As the fourth-order approximations of the vorticity equation are stable, the inner iterations are convergent for all values of Re.

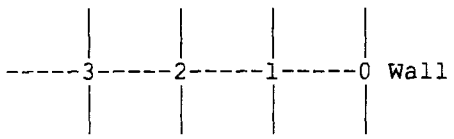

FIG. 3. Computational stencil for wall vorticity.

TABLE I

Representative Parameters of Driven Cavity (Fourth-Order Velocities, 41×41 Mesh)

	Primary vortex		Secondary vortices		
Re	ψ_{VC}	ζ_{VC}	ψ_{UVC}	ψ_{DVC}	$\zeta(0.5,1)$
1	0.100027	3.33906	$-0.2091(-5)^a$	$-0.2100(-5)$	5.8637
10	0.100029	3.35029	$-0.2212(-5)$	$-0.2011(-5)$	5.8686
100	0.103463	3.28572	$-0.1245(-4)$	$-0.1747(-5)$	6.5505
400	0.112814	2.30247	$-0.6512(-3)$	$-0.1452(-4)$	10.0856
1000	0.111492	2.02763	$-0.1823(-2)$	$-0.1491(-3)$	15.9470
2000	0.099586	2.24579	$-0.2849(-4)$	$-0.7597(-4)$	18.5790

$^a -0.2091(-5) = -0.20991 \times 10^{-5}$.

We obtained numerical solutions of the driven cavity problem for Reynolds numbers ranging between 1 and 2000. The solutions were obtained on a 21×21 grid ($h = \frac{1}{20}$) and a 41×41 grid ($h = \frac{1}{40}$). All iterations were started with zero initial data and were terminated when the maximum difference between successive approximations of ψ, ζ was smaller than 10^{-4}. The computations were carried out on an IBM 4381 at The George Washington University and on a CRAY XMP24 at NASA Lewis Research Center.

In Table I, we present the representative parameters of the driven cavity problem for the 41×41 grid, obtained using the fourth-order approximations (12) for the velocities. This table contains the values of ψ, ζ at VC (VC = center of the primary vortex), the values of ψ at the centers of the secondary vortices in the lower corners, and the value of ζ at the mid-point (0.5,1) of the moving wall. These parameters are the major indicators of the accuracy of the computed solutions [11] and are quoted by most authors.

We also computed numerical solutions using the second-order approximations (11) for the velocities. The solutions for $\mathrm{Re} = 1,10$ were found to be almost identical with those obtained using the fourth-order approximation for the velocities. The representative parameters using second-order velocities for $\mathrm{Re} \geqslant 100$ are given in Table II.

TABLE II

Representative Parameters of Driven Cavity (Second-Order Velocities, 41×41 Mesh)

	Primary vortex		Secondary vortices		
Re	ψ_{VC}	ζ_{VC}	ψ_{UVC}	ψ_{DVC}	$\zeta(0.5,1)$
100	0.103263	3.28369	$-0.1241(-4)$	$-0.1742(-5)$	6.5641
400	0.111151	2.29561	$-0.7004(-3)$	$-0.1367(-4)$	10.1538
1000	0.107392	2.01499	$-0.2108(-2)$	$-0.1384(-3)$	16.2462
2000	0.088152	2.37916	$-0.1368(-4)$	$-0.7979(-4)$	20.6838

Comparison with Existing Solutions

We now present a comparison of our solutions with the high accuracy solutions available in the literature (see, for example [7, 8, 17]). Qualitatively, our solutions exhibit the well-known features of the driven cavity, including the main vortex in the central part of the cavity and secondary vortices in the lower corners. Figures 4–7 present the streamfunction and vorticity contours for $\mathrm{Re} = 1$ and 100 using the $O(h^4)$ approximation for velocities. Figures 8–11 contain the streamfunction and vorticity contours for $\mathrm{Re} = 400$ using $O(h^2)$ and $O(h^4)$ approximations for velocities. Figures 12–15 contain similar contours for $\mathrm{Re} = 1000$. It is apparent that our streamfunction and vorticity contours are consistent with the published data [5, 7, 8, 17, 18].

Quantitatively, our solutions using the 41×41 mesh compare very well with the highly accurate benchmark solutions available in the literature. In Table III, we compare the values of streamfunction ψ at VC and the location of VC with the results from [7, 8, 17] as applied to the driven cavity configuration shown in Fig. 3. We note that the locations of the vortex center VC using fourth-order approximations for the velocities are within the cellwidth h ($h = 0.025$) of the reference data.

Taking the results of Ghia *et al.* [7] as the benchmark solutions, we compute the relative errors of the ψ values at VC for the solutions obtained by us, by Goodrich and Soh[8], and by Schreiber and Keller [17]. This data, given in Table IV, shows that our solutions obtained using fourth-order approximations for the velocities are either comparable in accuracy or are somewhat more accurate than the other results.

The values of streamfunction ψ at the center of the secondary vortex in the upstream corner UVC (in bottom left corner of the cavity, see Fig. 3) are given in

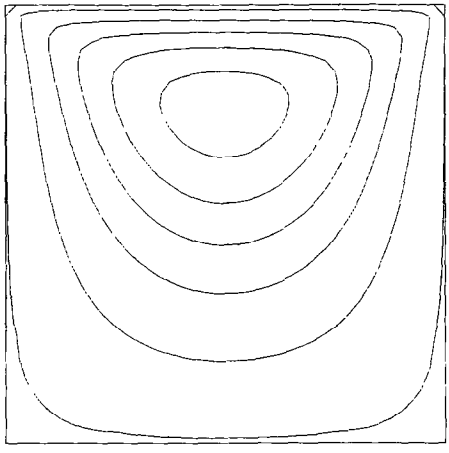

FIG. 4. Streamlines for $\mathrm{Re} = 1$ (fourth-order velocity).

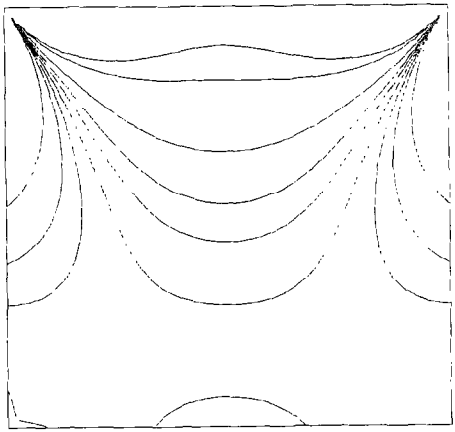

FIG. 5. Equivorticity curves for Re = 1 (fourth-order velocity).

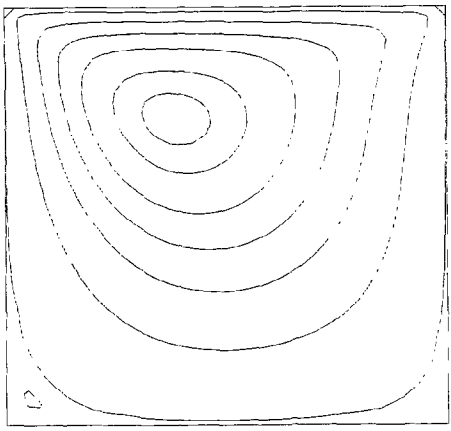

FIG. 6. Streamlines for Re = 100 (fourth-order velocity).

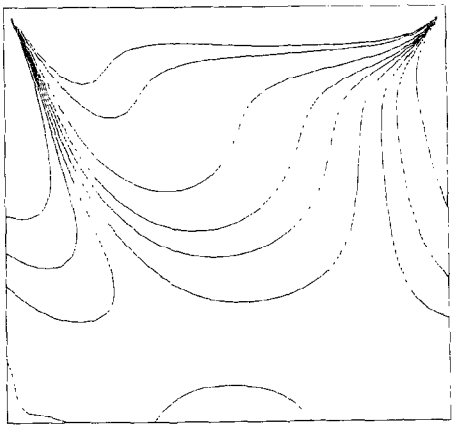

FIG. 7. Equivorticity curves for Re = 100 (fourth-order velocity).

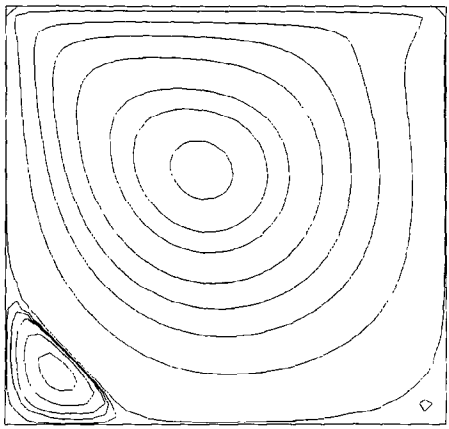

FIG. 8. Streamlines for Re = 400 (fourth-order velocity).

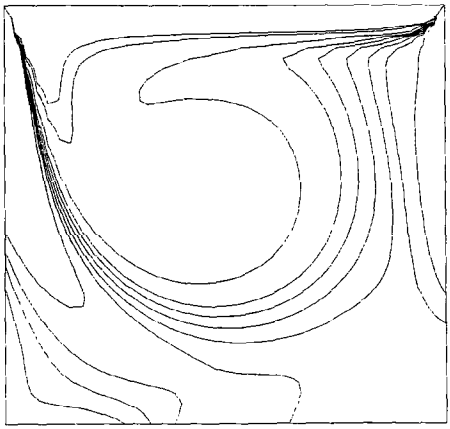

FIG. 9. Equivorticity curves for Re = 400 (fourth-order velocity).

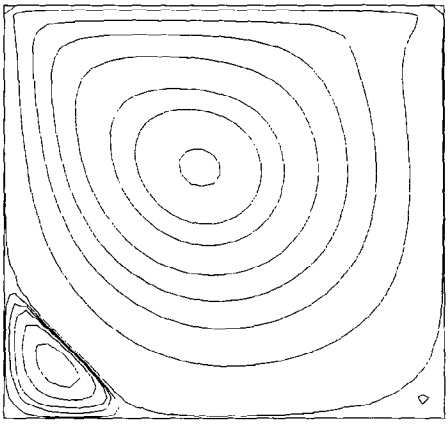

FIG. 10. Streamlines for Re = 400 (second-order velocity).

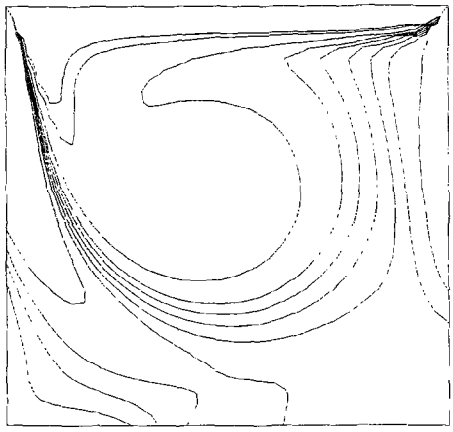

FIG. 11. Equivorticity curves for Re = 400 (second-order velocity).

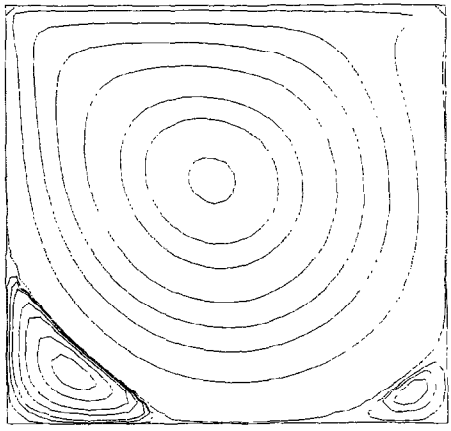

FIG. 12. Streamlines for Re = 1000 (fourth-order velocity).

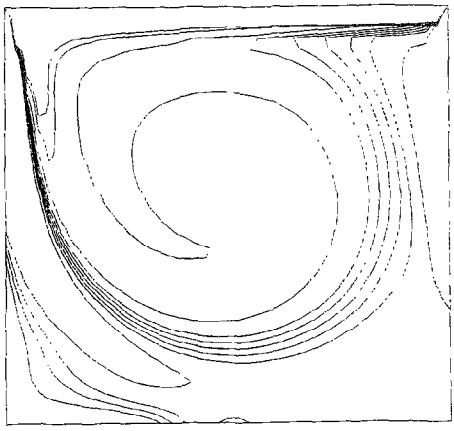

FIG. 13. Equivorticity curves for Re = 1000 (fourth-order velocity).

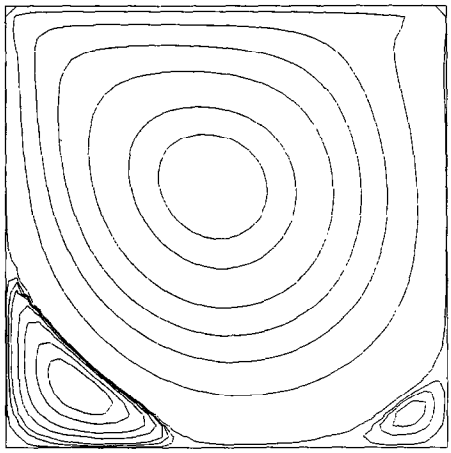

FIG. 14. Streamlines for Re = 1000 (second-order velocity).

Table V. We also give the reference data from [7, 8, 17] for comparison. The values of this parameter obtained using the fourth-order velocity approximations are much more accurate than those obtained using the second-order velocity approximations; at large values of Re, the improvement becomes even more pronounced.

In Table VI, we given the values of ζ at VC and compare with the available data. The agreement with the reference data is quite good even though the location of VC substantially effects the values of this parameter; smaller values of h would locate VC more accurately and give even better agreement in the ζ values at VC. In Table VII, we give the values of ζ at the mid-point of the sliding wall $y = 1$ and the only comparison data available in [7].

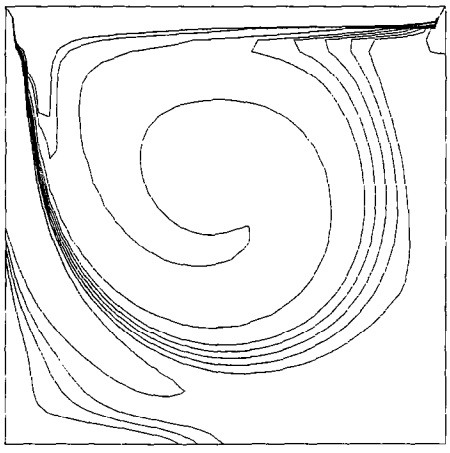

FIG. 15. Equivorticity curves for Re = 1000 (second-order velocity).

TABLE III

Value of ψ at VC and Location of VC (VC = Center of Primary Vortex)

Re	Second-order velocities	Fourth-order velocities	Reference data	
1	0.100027 (0.5, 0.775)	0.100027 (0.5, 0.775)	0.10006 (0.5, 0.7667)	[17]
100	0.103263 (0.375, 0.75)	0.103463 (0.375, 0.75)	0.103423 (0.3828, 0.7344)	[7]
			0.10330	[17]
400	0.111152 (0.45, 0.625)	0.112814 (0.45, 0.60)	0.113909 (0.4453, 0.6055)	[7]
			0.11198	[8]
			0.11297	[17]
1000	0.107392 (0.475, 0.600)	0.111492 (0.475, 0.575)	0.117929 (0.4687, 0.5625)	[7]
			0.11359	[8]
			0.11603	[17]

TABLE IV

Relative Error in the Value of ψ at VC

Re	Second-order velocities (%)	Fourth-order velocities (%)	Reference data (%)	
100	0.15	0.04	0.12	[17]
400	2.4	0.96	0.82	[17]
			1.7	[8]
1000	8.9	5.4	1.6	[17]
			3.7	[8]

TABLE V

Value of ψ at UVC (UVC = Center of Upstream Corner Vortex)

Re	Second-order velocities	Fourth-order velocities	Reference data	
1	$-0.2091(-5)$	$-0.2091(-5)$	$-0.247\ (-5)$	[17]
100	$-0.1241(-4)$	$-0.1245(-4)$	$-0.1254(-4)$	[7]
			$-0.1320(-4)$	[17]
400	$-0.7004(-3)$	$-0.6512(-3)$	$-0.6424(-3)$	[7]
			$-0.5749(-3)$	[8]
			$-0.6440(-3)$	[17]
1000	$-0.2108(-2)$	$-0.1833(-2)$	$-0.1751(-2)$	[7]
			$-0.1892(-2)$	[8]
			$-0.1700(-2)$	[17]

TABLE VI

Value of ζ at VC

Re	Second-order velocities	Fourth-order velocities	Reference data	
1	3.339	3.339	3.232	[17]
100	3.284	3.286	3.167	[7]
			3.182	[17]
400	2.296	2.302	2.295	[7]
			2.281	[17]
1000	2.015	2.028	2.050	[7]
			2.026	[17]

TABLE VII

Value of ζ at (0.5,1)

Re	Second-order velocities	Fourth-order velocities	Reference data	
1	5.8637	5.8637	—	
100	6.5641	6.5505	6.5745	[7]
400	10.1538	10.0856	10.0545	[7]
1000	16.2462	15.9470	14.8901	[7]

TABLE VIII

Extreme Value of Horizontal Velocity u at Centerline $x = 0.5$ near the Bottom Wall $y = 0$

Re	Second-order velocities	Fourth-order velocities	Reference data	
1	0.2065	0.2070	—	
100	0.2212	0.2223	0.2109	[7]
	(4.9%)	(5.4%)		
400	0.3235	0.3288	0.3273	[7]
	(1.2%)	(0.46%)	(2.2%)	[8]
1000	0.3473	0.3596	0.3829	[7]
	(9.3%)	(6.1%)	(4.6%)	[8]

TABLE IX

Extreme Value of Vertical Velocity v at Centerline $y = 0.5$ near the Left Wall $x = 0$

Re	Second-order velocities	Fourth-order velocities	Reference data	
1	−0.1678	−0.1685	—	
100	−0.2263	−0.2289	−0.2453	[7]
	(7.8%)	(6.7%)		
400	−0.4022	−0.4203	−0.4499	[7]
	(10.6%)	(6.6%)	(1.6%)	[8]
1000	−0.4188	−0.4522	−0.5155	[7]
	(18.7%)	(12.3%)	(3.9%)	[8]

In Table VIII, we give the extreme values of the horizontal velocity u at the centreline $x = 0.5$ near the bottom wall $y = 0$. Data from [7] and relative deviation of our results from this data is given for $\mathrm{Re} \geqslant 100$; also given is the relative error data from [8] for $\mathrm{Re} = 400$ and 1000. Similar data is given in Table IX for the extreme values of the vertical velocity v at the centreline $y = 0.5$ near the left wall $x = 0$. We observe that our extreme u values (Table VIII) are comparable to those of [8] although our extreme v values (Table IX) are somewhat more erroneous than those of [8].

In Table X, we compare the values of ψ and ζ at VC obtained with the 21×21 and 41×41 grids and note that the values of these parameters rapidly approach the benchmark values when the grid is refined. The rate of convergence is somewhat slower when Re is large. It is expected that on further grid refinement, the solutions for large Reynolds numbers would also exhibit rapid convergence.

TABLE X

Comparison of 21×21 and 41×41 Solutions

	Re	21×21 solution	41×41 solution	Reference data	
ψ_{VC}	1	0.099994	0.100027	0.10006	[17]
	100	0.103168	0.103463	0.103423	[7]
	400	0.101073	0.112814	0.113909	[7]
	1000	0.084237	0.111492	0.117929	[7]
ζ_{VC}	1	3.0294	3.3391	3.232	[17]
	100	3.1112	3.2857	3.1665	[7]
	400	2.3784	2.3025	2.2947	[7]
	1000	3.0194	2.0276	2.0497	[7]

Note. ψ, ζ at the center of the primary vortex (fourth-order velocities).

DISCUSSION

We note that for moderate values of the Reynolds number Re, the numerical solutions obtained using our high order compact difference approximations are highly accurate and compare well with the benchmark solutions available in the literature. This fact is remarkable also due to the fact that our solutions are obtained with a relatively coarse grid ($h = \frac{1}{40}$), whereas the benchmark solutions have been obtained with fine grids (with h as small as $h = \frac{1}{256}$).

In Table XI, we give the number of iterations needed to converge to the required tolerance. As expected, for larger values of Re the convergence is slower; however, the convergence is faster with the fourth-order velocity approximations than with the second-order velocity approximations. We also give the CPU execution times for $\mathrm{Re} = 1000$, 2000 on a CRAY XMP24 in this table. With $\mathrm{Re} = 1000$, the convergence with fourth-order velocity approximations required almost 13% less CPU time than with the second-order velocity approximations; with $\mathrm{Re} = 2000$ the discrepancy increased even further. Thus, the numerical computations using the second-order velocity approximations have slower convergence and produce less accurate results than the computations using the fourth-order velocity approximations.

We conclude that the fourth-order approximations for the Navier–Stokes equations do provide highly accurate solutions when coupled with appropriate high order approximations for the velocities. The rate of convergence of the outer iterations slows down considerably when computing for larger values of Re. This is an on-going difficulty with all solution methods. We are currently investigating alternative methods such as the multigrid and multilevel techniques [7, 20, 22] to obtain high accuracy driven cavity solutions for much larger values of Re and to solve other problems of viscous fluid flow. The results of these investigations shall be reported in the future.

TABLE XI

Number of Outer Iterations, CPU Execution Times to Converge to 10^{-4} (CRAY XMP24)

Re	Second-order velocities	Fourth-order velocities
1	157	157
100	353	353
400	516	509
1000	1248 (148 s)	1040 (127 s)
2000	>6200 (>645 s)	4266 (482 s)

REFERENCES

1. A. BERGER, J. M. SOLOMON, M. CIMENT, S. H. LEVENTHAL, AND B. C. WEINBERG, *Math. Comp.* **35**, 695 (1980).
2. G. BIRKHOFF AND R. E. LYNCH, *Numerical Solution of Elliptic Equations* (SIAM, Philadelphia, 1984).
3. L. COLLATZ, *The Numerical Treatment of Differential Equations* (Springer-Verlag, Berlin/New York, 1960).
4. C. J. FREITAS, R. L. STREET, A. N. FINDIKAKIS, AND J. R. KOSEFF, *Int. J. Numer. Methods Fluids* **5**, 561 (1985).
5. C. J. FREITAS AND R. L. STREET, *Int. J. Numer. Methods Fluids* **8**, 769 (1988).
6. J. S. B. GAJJAR, *Comput. Phys. Commun.* **37**, 303 (1985).
7. U. GHIA, K. N. GHIA, AND C. T. SHIN, *J. Comput. Phys.* **48**, 387 (1982).
8. J. W. GOODRICH AND W. Y. SOH, *J. Comput. Phys.* **84**, 207 (1989).
9. G. GUJ AND F. STELLA, *Int. J. Numer. Methods Fluids* **8**, 405 (1988).
10. M. M. GUPTA, *J. Comput. Phys.* **55**, 166 (1984).
11. M. M. GUPTA AND R. MANOHAR, *J. Comput. Phys.* **31**, 265 (1979).
12. M. M. GUPTA, R. MANOHAR, AND J. W. STEPHENSON, *Int. J. Numer. Methods Fluids* **4**, 641 (1984).
13. M. M. GUPTA, R. MANOHAR, AND J. W. STEPHENSON, *Num. Methods Partial Diff. Equations* **1**, 71 (1985).
14. R. E. LYNCH AND J. R. RICE, *Proc. Nat. Acad. Sci.* **75**, 2541 (1978).
15. R. MANOHAR AND J. W. STEPHENSON, *SIAM J. Sci. Statist. Comput.* **5**, 69 (1984).
16. P. J. ROACHE, *Computational Fluid Dynamics* (Hermosa, Albuquerque, NM, 1973).
17. R. SCHREIBER AND H. B. KELLER, *J. Comput. Phys.* **49**, 310 (1983).
18. W. A. SHAY, *Comput. Fluids* **9**, 279 (1981).
19. J. W. STEPHENSON, *J. Comput. Phys.* **55**, 65 (1984).
20. S. P. VANKA AND K. P. MISEGADES, *Int. J. Numer. Methods Fluids* **7**, 635 (1987).
21. S. C. R. DENNIS AND J. D. HUDSON, *J. Comput. Phys.* **85**, 390 (1989).
22. M. C. THOMPSON AND J. FERZIGER, *J. Comput. Phys.* **82**, 94 (1989).